

## SUPPRESSION OF HELIUM BUBBLE GROWTH IN FRICTION STIR WELDING OF IRRADIATED MATERIALS – Zhili Feng and Stan A. David (Oak Ridge National Laboratory)

### OBJECTIVE

To conduct preliminary assessment on the potential benefits of friction stir welding process in welding repair of irradiate materials.

### SUMMARY

Computational simulations were conducted to investigate the helium bubble growth during friction stir welding of irradiated stainless steel. The helium bubble evolution model by Kawano et al was incorporated into the finite element based welding temperature and stress computational model to obtain the temporal and spatial distribution of the helium bubbles in the heat-affected zone of a weld. The predicted maximum helium bubble location in a gas tungsten arc weld correlated very well with the actual helium induced cracking site. The compressive thermal stress, coupled with the lower temperature, of the friction stir welding process inhibits the helium bubble growth. The calculations show that, even without fine-tuning the FSW process parameters, the maximum helium bubble size in a friction stir weld is only about 27% of a gas tungsten arc weld of comparable size. This preliminary study suggests that friction stir welding is advantageous in circumventing the helium induced cracking for welding of irradiated materials.

### PROGRESS AND STATUS

#### Introduction

Fusion welding of irradiated materials has been difficult. Depending on the level of irradiation, welding can result in cracking in the heat-affected zone (HAZ) of the weld region [1]. The cracking is attributed to the entrapped helium in the post-irradiated material [2,3]. The helium bubbles nucleate, grow and coalesce rapidly at grain boundaries under the high temperature and tensile stresses in welding. Intergranular brittle rupture occurs as the cohesive strength of the grain boundary (weakened by helium bubbles) can no longer bear the tensile stress caused by the cooling contraction of the weld. In principle, the formation of He bubble and the He induced cracking can be inhibited or eliminated by minimizing the exposure to tensile stresses at elevated temperatures [4]. However, eliminating the tensile stress in a fusion welding process is very challenging in practice, if impossible.

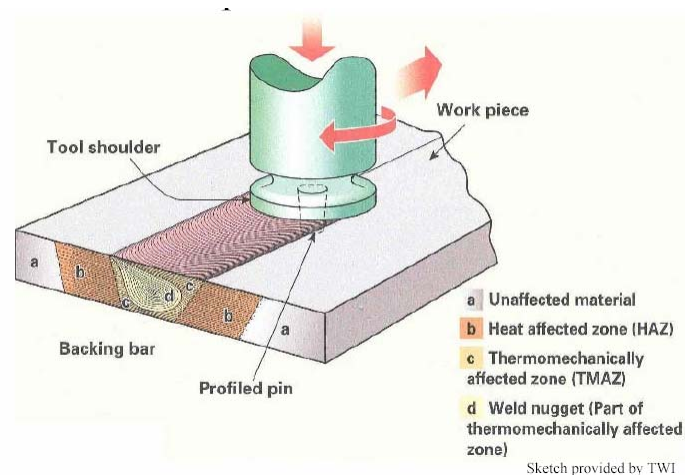


Figure 1 Schematics of Friction Stir Welding Process

Friction stir welding (FSW) is a new, innovative solid-state joining process developed in the 1990s [5]. As shown in Figure 1, the process utilizes a rotating tool to generate heat to soften the material which is then mechanically stirred and consolidated to form the metallurgical bond. To date, the FSW has been

successfully used for high-strength aluminum alloys that are considered non-weldable with fusion welding processes because of solidification related defects. Although many challenging technical issues still remain, friction stir welding of high-melting temperature materials such as stainless steels and Ti alloys has demonstrated feasible [6].

### Approach

Experimentally making friction stir weld on irradiated materials is very costly and time-consuming. As a feasibility study, we utilized the advanced welding simulation models to investigate the formation of He bubble during friction stir welding. For comparison, we also analyzed the formation of He bubble in gas tungsten arc welding (GTAW) process reported from the literature [7].

### Materials and Welding Conditions

The materials, specimen geometry, and welding conditions for the GTAW process followed those of the experimental weldability study by Asano et al [7]. The irradiated SS 304 stainless steel plate was autogenously welded at a heat input level of 7.1kJ/cm. The plate was 8-mm thick, 30-mm wide, and 60-mm long. The weld appearance is shown in Figure 2. The He-induced cracks are also apparent in the figure. The cracks are predominately around the bottom of the weld.

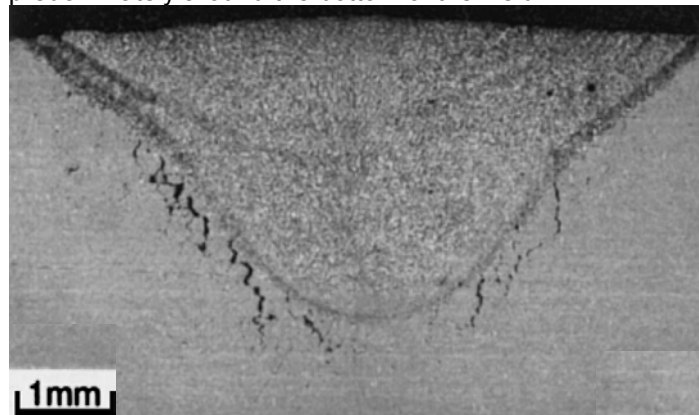


Figure 2 Appearance of helium-induced cracks from Asano's study [7].

For the friction stir weld, the process conditions were selected such that the anticipated weld depth and width would be similar to those of the GTA weld by Asano et al. Key process parameters were  $\frac{3}{4}$ " shoulder diameter, 530 rpm rotational speed, and 3 in/min welding travel speed.

Asano reported an initial He concentration of 8.3 appm, but did not report the He bubble size in their test. In this work, the initial He concentration was increased to 100 appm, such that the predicted helium bubble growth could be verified against Hashimoto's work [8].

### Modeling of Temperature and Thermal Stress in Welding

The weld plate was modeled as a two-dimensional cross-section model. The generalized plain strain formulations were used to deal with the out-of-plane bending due to the thermal expansion. The welding was modeled as a transient non-linear thermo-mechanical deformation process, with temperature dependent material properties. The effects of solidification on the thermal stress field at elevated temperatures were considered following the approach developed previously [9]. This type of model has been widely used for simulating the temperature and stress evolutions associated with long and straight weld.

For the GTAW process, the welding heat input took the ellipsoidal form.

$$q = \frac{6\sqrt{3}\eta EI}{\pi\sqrt{\pi abc}} e^{\left[-3\left(\frac{x^2}{a^2} + \frac{y^2}{b^2} + \frac{z^2}{c^2}\right)\right]} \quad (1)$$

where E and I are the welding voltage and current respectively. The arc efficiency,  $\eta$ , is assumed to be 70% for the GTA welding process. The parameters a, b, and c are related to characteristics of the welding arc. In this equation, the origin of the coordinate system is located at the center of the welding arc.

For the FSW process, the heat generation was assumed to be from the surface friction between the tool shoulder and material, and took the following form:

$$q = \frac{3\eta T\omega}{2\pi R^3} r \quad (2)$$

where r is the radial distance from the center of the tool, T the torque,  $\omega$  the rotational speed, R the radius of the tool shoulder.

#### *Modeling of Helium Bubble Evolution*

Although more elaborate models available (such as these by Hashimoto et al [8]), we choose to implement the one by Kawano et al [10] for its simplicity in this preliminary phase of study. Kawano's equations are an extension of the work by Grossback et al [3]. We numerically integrated the set of differential equations by Kawano over the entire welding thermal and stress cycle at every integration point of the finite element model, to obtain the temporal and spatial distribution of the helium bubble.

The helium bubble outside the fusion zone was simulated according to Kawano's equations. On the other hand, the helium bubble inside the molten weld pool involves different mechanisms. For example, helium bubble would escape from the weld pool as a result of molten metal flow and transport. Therefore, the helium bubble inside the fusion zone was artificially assumed to be completely escaped, thereby having zero radius and density.

## **Results**

#### *Helium Bubble in GTA weld*

Figure 3 shows the predicted distribution of helium bubble size (radius). Outside the fusion zone, significant helium bubble growth only occurs in a narrow band of about 1-mm wide adjacent to the fusion line where the peak temperature reaches the melting point of the material. The bubble grows negligibly if the peak temperature is below 1000K. Within this band, the helium bubble is considerably smaller near the surface of the plate, suggesting the important influence of the stress state. Finally, the predicted maximum helium bubble locations are in very good agreement with the observed cracking sites, indicating the validity of the model.

The predicted final maximum helium bubble radius is about 252 nm. Quantitatively, this prediction is about an order of magnitude smaller than these with simplified stress assumptions [3]. But it agrees with these using more realistic welding temperature and stress conditions [8] and experimental observations of welds made with similar welding conditions and helium concentrations.

#### *Helium Bubble in Friction Stir Weld*

Figure 4 show the predicted distribution of final helium bubble radius in the friction stir weld. For reference, the geometry of the FSW tool is superimposed onto the FSW case, and the weld bond region is also highlighted. The result of the GTAW is also plotted next to the FSW which provides direct visual comparisons of the weld shape and he bubble distribution.

As shown in Figure 4, the friction stir weld has similar depth to that of the GTA weld, but is wider near the plate surface due to the heating of the tool shoulder. The growth of the helium bubble is substantially suppressed – the maximum bubble radius of the FSW case is about 69 nm, which is only 27% of the maximum bubble radius in the GTAW case. Analyses of the simulation data suggested that this is primarily due to fact that the hot stirred region subjects to a compressive hydraulic pressure from the tool shoulder.

It should be noted that the selected FSW conditions was based on the previous experience in making friction stir weld in stainless steels. They could be improved to further lower the temperature during the process, and the tool geometry could be refined to maximize the benefits of the compressive stress.

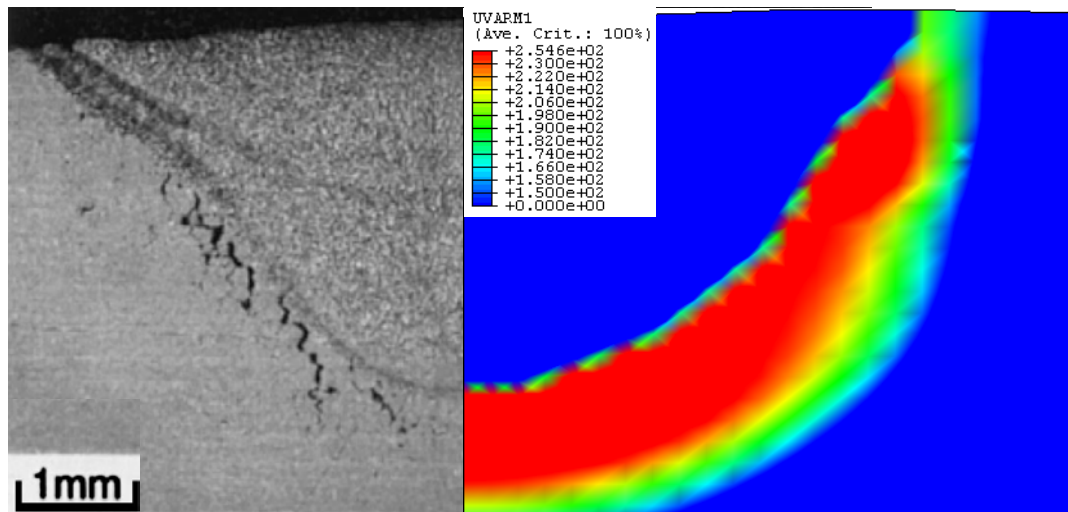


Figure 3 Predicted helium bubble radius in relation to the observed weld shape and location of He induced cracks. He bubble radius in nm.

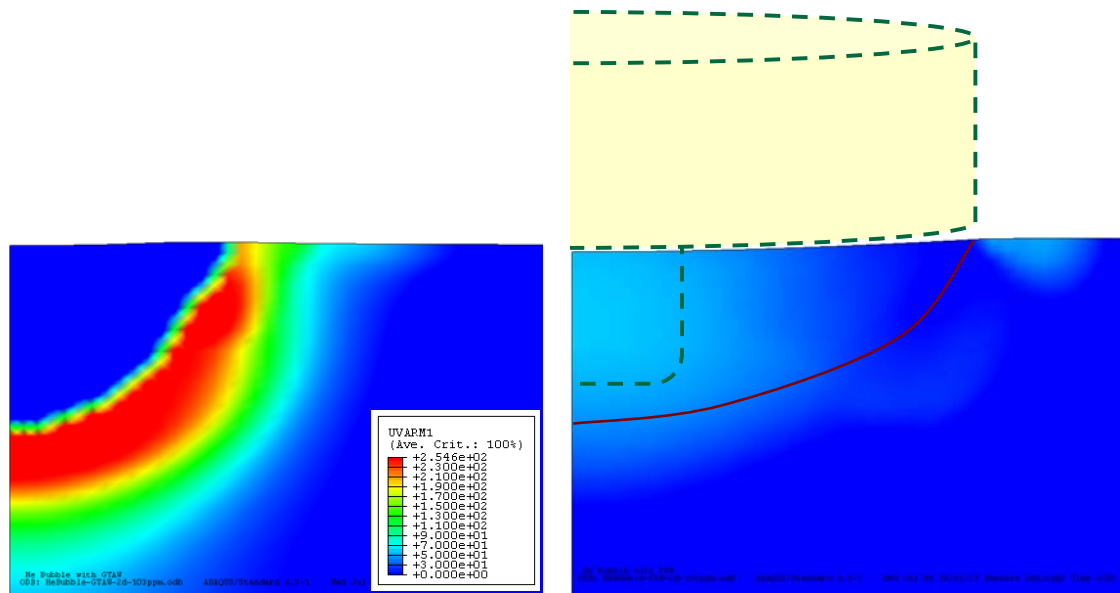


Figure 4 Comparison of helium bubble radius in FSW against GTAW. The GTA weld is on the left, whereas the friction stir weld is on the right.

## References

- 1 Maloney, J.P., Baker, D, Kennedy, W.R., Day, W.A., McClain, J.B., Fraser, W.G, McKenney, D.H, Huxford, H.R., Meyer, C.A., Kehr, K.E., Mittelberg, R.F., and Walls, J.E., 1969, "Repair of a Nuclear Reactor Vessel," AEC R&D Report, Savannah River Laboratory, DP-1199.
- 2 Kanne Jr., W.R., 1988, "Remote reactor repair: GTA weld cracking caused by entrapped helium," *Welding Journal*, **67**, pp. 33-39.
- 3 Lin, H.T, Grossbeck, M.L. and Chin, B.A., 1990, "Cavity microstructure and kinetics during gas tungsten welding of helium-containing stainless steel," *Metall. Trans.* **21A**, pp. 2585-2596.
- 4 Kanne Jr., W.R., Chandler, G.T., Nelson, D.Z. and Franko-Ferreira, E.A., 1995, "Welding irradiated stainless steel," *J. Nuclear Materials*, **225**, pp. 69-75.
- 5 Thomas, W.M., Nicholas, E.D., Needham, J.C., Murch, M.G., Temple-Smith, P. and Dawes, C.J. 'Improvements relating to friction stir welding', European Patent Specification 0615480 B1, 1991.
- 6 Gould, J.E., Lienert, T.J. and Feng, Z., 1998, "Recent developments in friction stir welding," SAE Technical Paper Series 981875.
- 7 Asano, K., Nishimura, S., Saito, Y., Sakamoto, H., Yamada, Y., Kota, T. and Hashimoto, T., 1999, "Weldability of neutron irradiated austenitic stainless steels," *J. Nuclear Materials*, **264** pp 1-9.
- 8 Hashimoto, T. and Mochizuki, M., 1999, "Modeling of helium bubble formation during welding of irradiated stainless steels," *Proc. 19<sup>th</sup> Int. Sym. Effects of Radiation on Materials*, ASTM STP 1366. Hamilton M.L. et al. eds. ASTM.
- 9 Feng, Z. 1994, "A computational analysis of thermal and mechanical conditions for weld metal solidification-cracking," *Welding in the World*, **33**(5) pp. 340-347.
- 10 Kawano, S., Sumiya, R. and Fukuya, K, 1998, "Simulation of helium bubble behavior in neutron-irradiated stainless steel during welding," *J. Nuclear Materials*, **258-263** pp. 2008-2012.